ELSEVIER

Agricultural and Forest Meteorology 87 (1997) 223–241

AGRICULTURAL AND FOREST METEOROLOGY

Estimation of maximum possible daily global solar radiation

David W. Meek *

USDA-Agricultural Research Service, National Soil Tilth Laboratory, 2150 Pammel Drive, Ames IA 50011, USA

Received 29 August 1996; recieved in revised form 26 February 1997; accepted 10 March 1997

Abstract

The estimation of maximum possible daily global solar radiation is important in many applied sciences. This study develops and evaluates climatic extreme based modifications of two single-atmospheric-layer broadband solar shortwave irradiance models for the purpose of estimating a dynamic upper boundary for global solar radiation at any given location. Climatic component models were developed for five rural locations in the central United States: Ames, IA, Bismarck, ND, Columbia, MO, Dodge City, KS, and Wooster, OH. Each site had long-term (30 or 31 years) records of daily global solar radiation data available. Aerosol optical depth, precipitable water, and surface albedo were the input variables. Data for the first two inputs were obtained from the SAMSON database (Solar and Meteorological Observation Network). Albedo interpolating curves were estimated from the predecessor of SAMSON. For each site, precipitable water and aerosol optical depth daily data were used to develop annual trends in the climatic lows and normals for each variable. The normals were based on median daily values. Nonlinear generalized least squares regression analyses were used to develop the interpolating curves. To evaluate the global radiation models, maximum daily global solar radiation values were selected for each day in the year from the entire period of record for each site. In either broadband model, the use of the climatic normals in each input variable either interpolated or underestimated the selected radiometer data. The use of the climatic lows, however, yielded a reasonable upper boundary for the selected data. The result may be partially due to the fact that the climatic minima curves for each turbidity variable were generally significantly different throughout the year from the climatic normals ($P < 0.05$). The global solar radiation models were most sensitive to aerosol optical depth. Although it is more sensitive to input variation and it is somewhat less conservative, the simpler of the two broadband models is adequate for most applications. While results are site-specific, the methodology is general and provides a climatic-based definition for maximum possible daily global solar radiation. Published by Elsevier Science B.V.

Keywords: Global radiation models; Solar radiation; SAMSON database; Albedo; Turbidity

1. Introduction

Estimation of maximum possible daily global solar radiation at the earth's surface is needed for agronomic modeling and managerial purposes (see Davies and Idso, 1979; Howell et al., 1983, 1984; Jensen et al., 1990).

* Corresponding author. Tel.: + 1-515-294-2246; fax: + 1-515-294-8125; e-mail: MEEK@NSTL.GOV

0168-1923/97/$17.00 Published by Elsevier Science B.V.
PII S0168-1923(97)00025-7

Furthermore, other biological, climatic, environmental, hydrological, solar energy, and engineering applications need such an estimate (see Brutsaert, 1982; Iqbal, 1983; Tracy et al., 1983). Ångström (1924) may have been the first to introduce the concept; he referred to it as the "radiation income on a perfectly clear day for the duration of the day".

One emerging application is for the quality control of data in a micrometeorological database. For multiple uses, solar radiation is increasingly being measured in agricultural weather data networks (e.g., see Meyer and Hubbard, 1992; Snyder and Pruitt, 1992). Meek and Hatfield (1994) propose screening daily global solar radiation data, $R_s(d)$, with a dynamic upper boundary often called a 'clear day curve', $R_{s,c}(d)$, which should equal the maximum possible daily value for the measurement [1]. For each daily datum, $R_s(d) \leq R_{s,c}(d)$. An empirical sinusoidal regression curve, Eq. (1) on p. 90, was developed from the maximum daily datum over a 31-year period of record for daily R_s data. An analogous rule for hourly data was proposed based on using the hourly extraterrestrial value as an upper bound. An anonymous reviewer for the journal article wanted such rules to be based on an atmospheric radiative transfer model.

In addition to screening R_s data, there is another need for $R_{s,c}$. It can be used in energy balance modeling and its application to evapotranspiration estimation for irrigation scheduling. Models use $R_{s,c}$ for estimating global solar radiation (R_s), net longwave radiation ($R_{l,n}$), and surface net radiation (R_n). Brutsaert (1982) discusses the use of $R_{s,c}(d)$ in the estimation of $R_s(d)$ when measurements are unavailable, but he advises caution since the models are still experimental and development is still underway (see Eqs. 6.3–6.5 in Brutsaert, 1982). Jensen et al. (1990) also discuss the various parameterizations in Chapter 3 (see Eqs. 3.1–3.3b in Jensen et al., 1990). In some applications estimating $R_{s,c}(d)$ is abandoned and parameterizations based on extraterrestrial solar radiation are used (see e.g., Eq. (4.2.6) in Shuttleworth, 1993 or Eq. (3.27) in Hatfield and Fuchs, 1990). The extraterrestrial parameterizations are used because a reasonable $R_{s,c}$(d) estimate is difficult to calculate. Also, there may not be a locally derived empirical model available.

When $R_s(d)$ data are available but net radiation data are not, the $R_{l,n}(d)$ can be modeled using $R_{s,c}(d)$ estimates. A common $R_{l,n}(d)$ parameterization uses a cloudiness factor, f, where $f = a(R_s(d)/R_{s,c}(d)) + b$ with a and b defined as locally determined empirical longwave radiation coefficients (see e.g., Eq. (4.2.10) in Shuttleworth, 1993; Eqs. (3.15) and (3.16) in Jensen et al., 1990; or Eq. (2) in Heermann et al., 1985). For clear skies, $a + b = 1$. Ideally $(R_s(d)/R_{s,c}(d)) \leq 1$. Empirical models for $R_{s,c}(d)$ can be found in the agronomic literature (e.g., see Heermann et al., 1985; Fig. 4 in Howell et al., 1984; or Fig. 4 in Howell et al., 1983). Incidentally, in a work by Dong et al. (1992), an hourly parameterization for $R_s/R_{s,c}$, Eq. (11) of Dong et al., 1992, was developed for the estimation of hourly net radiation because, once again, $R_{s,c}$ is difficult to estimate. Also, there are some radiative transfer approaches to estimating $R_{s,c}$ (e.g., see Eqs. (3.3)–(11) in Davies and Idso, 1979; Tracy et al., 1983). This approach is not widely used and until now has required arbitrary and/or ad hoc turbidity estimates (see below).

Clear-day curves can be crudely inferred from charts in a solar atlas (e.g., see USDOE, 1978; Baker and Klink, 1975). Some are developed from site-specific long-term radiometer data, but such data are not widely available. Moreover, Meyer and Hubbard (1992) and Snyder and Pruitt (1992) list many automated stations that have recently come into operation and so have limited historical records. When long-term data are available, sinusoidal regression curves that interpolate these data have been used for estimating clear-day curves (e.g., see Meek and Hatfield, 1994; Heermann et al., 1985). Ideally, such a curve should not interpolate the data, but bound them in the mathematical sense of a least upper bound for each day in the year.

An alternative method would be to use radiative transfer models set for climatic extremes of favorable transmission conditions. Unfortunately, for spectral models, geographically representative data are not readily available. Conceptually, as a more practical alternative, clear-sky adaptations of single-atmospheric-layer

[1] Brutsaert (1982) denotes this term as R_{sc}. Jensen et al. (1990) denote it as R_{b0}. Meek and Hatfield (1994), among others, denote it as SI_c.

broadband shortwave radiative transfer routines (generally, 0.3–3.0 μm) similar to those of Atwater and Ball (1976) or Iqbal (1983) should be adequate, but their use has been limited because of required input data that are scarce or unavailable and had to be estimated in various, often indirect, ways (e.g., see Suckling and Hay, 1976; Meyers and Dale, 1983; Tracy et al., 1983). With the availability of the Solar and Meteorological Observation Network database (SAMSON) this situation has changed. To bring solar radiation data up to the 30-year WMO (1967) standard (and in cooperation with the US National Climatic Data Center [NCDC]), the US National Renewable Energy Laboratory (NREL, formerly SERI [Solar Energy Research Institute]) developed the National Solar Radiation Data Base (NRSDB) that is more commonly called the SAMSON database. It contains a serially complete quality controlled 30-year record that includes total and component shortwave irradiance data, as well as many other meteorological variables, all on an hourly basis, for 56 primary sites and 183 secondary sites (NREL, 1992, 1995). The SAMSON database radiation components at the primary stations are based, at least partially, on measurements, while corresponding data for the secondary stations are modeled. The production of the SAMSON database made use of the clear sky algorithms of Bird and Hulstrom (1981), with the exception of aerosol transmittance. Aerosol transmittance used a broadband form of Beer's Law.

The SAMSON database can be employed in a variety of useful ways including the previously mentioned data screening, global radiation, and surface energy balance applications used by a variety of research, public, and private sector organizations. Meyer and Hubbard (1992) reviewed the data needs and development of nonfederal weather station networks; Snyder and Pruitt (1992) reviewed evapotranspiration data needs for irrigation and drainage management; and some recent multiagency hydrological projects required short-term real-time meteorological data (e.g., see USDA, 1994; Kustas and Goodrich, 1994).

This study has two objectives, the second contingent upon the first. The first one is to find a nonarbitrary method to estimate maximum possible daily global solar radiation at any given arbitrary location. Ideally an appropriate model estimates the upper boundary for global radiometer data from an instrument set on a horizontal surface and for a cloud-free, clear, and dry atmosphere. The hypothesis is that a chosen broadband model will more reasonably bound selected clear day global radiometer observations using the trend in climatic lows for each of two turbidity inputs (precipitable water and aerosol optical depth) than it will by using the corresponding normal trends. To accomplish the task, I adapted two published hourly-based clear-sky single-atmospheric-layer broadband radiative transfer models for use with annual trend climatic component input models for the turbidity variables. If my hypothesis is sound, then with the use of the climatic low annual trends in the turbidity variables, an unambiguous definition and means of estimation emerges for 'a cloud-free, clear, and dry atmosphere'. Setting this climatic-based definition is my second objective.

2. Data

A summary of data used in this study is presented in Table 1. Aerosol optical depth, precipitable water, and albedo data were needed to develop the annual trend models that were to be used in the selected broadband global solar radiation models. Five small-town sites with rural surroundings were chosen where radiometer data were available, and climatic data needed for developing the annual trend component models were either available or could be interpolated from nearby locations. The sites chosen were Ames, IA, Bismarck, ND, Columbia, MO, Dodge City, KS, and Wooster, OH. Solar radiation and each of the climatic inputs can often reasonably be interpolated over large areas. Based on studies and theory, very clear day radiation should be uniform over wide areas, especially longitudinally in areas of low relief (Bland and Clayton, 1994). Flowers et al. (1969), Iqbal (1983), or NREL (1995) discuss variability in aerosol optical depth. NREL (1995) discusses variability in precipitable water. Hummel and Reck (1979) and Kung et al. (1964) discuss albedo variability. The daily Ames and Wooster global solar radiation data with limited additional meteorological data were obtained from the agricultural experiment stations in Iowa and Ohio. The SAMSON database and its predecessor, called the SOLMET database, were the data sources for the other three locations. These three

Table 1
Site geographic coordinates and data information

Site	Latitude	Longitude	Elevation	Data[a] type	Sources	Record period
Ames, IA	42.03°N	93.80°W	335.0 m	$R_s(d)$	ISU	31 yr
Akron, OH	40.92°N	81.42°W	377.0 m	$\sigma_a(d)$	SAMSON	30 yr
				$w(d)$	SAMSON	30 yr
Bismarck, ND	46.77°N	100.75°W	502.0 m	$R_s(d)$	SAMSON	30 yr
				$\sigma_a(d)$	SAMSON	30 yr
				$w(d)$	SAMSON	30 yr
				α(mon)	Iqbal, 1983	NA[c]
Columbia, MO	38.82°N	92.22°W	270.0 m	$R_s(d)$	SAMSON	30 yr
				$\sigma_a(d)$	SAMSON	30 yr
				$w(d)$	SAMSON	30 yr
				α(mon)	Iqbal, 1983	NA
Dodge City, KS	37.77°N	99.97°W	787.0 m	$R_s(d)$	SAMSON	30 yr
				$\sigma_a(d)$	SAMSON	30 yr
				$w(d)$	SAMSON	30 yr
				α(mon)	Iqbal, 1983	NA
Madison, WI	43.12°N	89.32°W	262.0 m	$\sigma_a(d)$	SAMSON	30 yr
				$w(d)$	SAMSON	30 yr
				α(mon)	Iqbal, 1983	NA
Omaha, NE	41.37°N	96.52°W	404.0 m	$\sigma_a(d)$	SAMSON	30 yr
				$w(d)$	SAMSON	30 yr
				α(mon)	Iqbal, 1983	NA
Toronto[d]	43.75°N	79.50°W	178.3 m	α(mon)	Iqbal, 1983	NA
Wooster, OH	40.78°N	81.92°W	310.9 m	$R_s(d)$	OSU	31 yr

[a] R_s is global solar radiation (MJ m^{-2}), σ_a is aerosol optical depth (dimensionless), w is precipitable water (cm), and α is albedo.
[b] ISU (Iowa State University); SAMSON (Solar And Meteorological Observation Network); and OSU (Ohio State University, a.k.a. OARDC).
[c] NA is not available.
[d] Canada.

selected SAMSON sites, Bismarck, Columbia, and Dodge City, are all well documented in the literature (e.g., see NREL, 1992, 1995; Baker and Klink, 1975; Iqbal, 1983). In addition, these sites were selected because they are primary stations which are located in mainly rural areas. Omaha, Madison, and Columbia were selected as the nearest primary stations for interpolating ancillary SAMSON data for use in the Ames broadband model. Akron/Canton was selected as a secondary SAMSON station that is nearest Wooster; so near that no interpolation schemes were needed.

2.1. Aerosol optical depth (σ_a)

A database for turbidity entirely founded on measurements was not possible because long-term records of turbidity measurements are spatially and temporally sparse. Hence, for the SAMSON database, Maxwell and Myers at the NREL developed a broadband turbidity surrogate (broadband aerosol optical depth-σ_a) based on Beer's Law applied to direct broadband atmospheric transmission (Chapter 6 of NREL, 1995). Beer's Law is strictly valid only for spectral losses from the beam; therefore, arguments and comparisons to spectral models are provided in the NREL documentation.

Since neither Ames nor Wooster were in the SAMSON database, to obtain σ_a for Ames, IA, data from the SAMSON primary stations at Omaha, NE (WBAN 94918), Columbia, MO (WBAN 03945), and Madison, WI (WBAN 14837) were averaged with inverse distance weights. The respective weights were 0.449, 0.279 and 0.272. Since all stations are within a 100-m (< 0.01 standard atmosphere) elevation difference from Ames, no elevation adjustments were made. While Des Moines, IA (the nearest station in the SAMSON database) is a nearby secondary station, the primary sites were deliberately selected. The criteria were: (1) the σ_a data were at least partially based on solar radiation measurements and (2) the resulting Ames σ_a model can then be compared to the model NREL developed for Des Moines (Appendix B, Table B1 of NREL, 1995). While data for Wooster could have been interpolated from the nearest primary stations, the direct use of data from the closest station was of obvious practical interest. Therefore, to test the direct use of data from a nearby secondary station, σ_a data from Akron/Canton, OH (WBAN 14895) were used for σ_a data at Wooster. Bismarck, Columbia, and Dodge City daily σ_a were directly used. In all cases, daily values were the same as the noontime hourly values.

2.2. Total precipitable water (w)

Surface dew point or humidity has been used to estimate w in broadband models (e.g., Meyers and Dale, 1983). Unfortunately, there are problems with this approach. Dew point or sounding data are often unavailable at some Class A or lower quality sites, especially some of those in the Cooperative State Network. Moreover Reber and Swope (1972) found that w is often poorly related to surface humidity. Without a sounding or other test the validity of the w estimate from the surface observation is unknown. Moreover, w was conveniently included in the meteorological data for the SAMSON database and was, therefore, directly used. Average daily w values over the 24-h period were computed from the hourly values for each of the chosen SAMSON sites. Estimation of the Ames daily w value followed the interpolating procedure used in estimating the daily Ames σ_a value.

2.3. Surface albedo (α)

Albedo data are not widely available. Interpolating values can present problems since local surface conditions could vary considerably, but in the absence of local data, there was no measurement-based alternative. Using data from SAMSON's predecessor, SOLMET, and other sources, Iqbal (1983) tabulates monthly means for numerous locations throughout the United States and Canada. No extremes or variations were given. Included were values for the three primary stations used to obtain the Ames σ_a values. The respective monthly α values at the primary sites and previously calculated weights were used to estimate monthly α values for Ames. Data for Wooster were interpolated from Columbia and Madison in the United States, and Toronto in Canada. Respective inverse distance-based weights were 0.122, 0.218 and 0.660. Data for Bismarck, Columbia, and Dodge City were the values tabulated in Iqbal (1983).

2.4. Global solar radiation (R_s)

The daily R_s data for Bismarck, Columbia, and Dodge City were chosen because network history, operations, instrumentation, changes, and calibrations associated with the data are well documented (Chapter 2 of NREL, 1995, 1993). The period of record was from 1961–1990. Corresponding data for Ames, IA recorded from 1960 through 1990 were obtained from the Iowa State University (ISU) Experiment Station. Similar data for Wooster, OH recorded from 1962 through 1992 were obtained from the nearby Ohio State University Experiment Station (OARDC). At both the ISU and OARDC sites an Eppley PSP pyranometer was used (spectral response, 0.285–2.800 μm) [2]. The Wooster radiometer was located on the OARDC farm. Additional information, especially for Wooster, was sparse. The Ames radiometer was located on the ISU Campus but was moved three

[2] Names are necessary to report factually on available data. However, the USDA neither guarantees nor warrants the standard of the product, and the use of the name by USDA implies no approval of the product to the exclusion of others that may also be suitable.

times during the period of record. Complete instrumentation and calibration history has not been formally summarized, but a brief assessment of the data quality was reported in Baker and Klink (1975). Until the early 1980s, data were recorded on strip charts, and daily values were obtained via planimetry. The methodology could have introduced a 5% or more error, possibly tending toward systematic overestimation of the daily values.

3. Methodology

Annual trend regression models for each site (i.e., depending only on day in the year) were developed to provide aerosol optical depth [$\sigma_a(d)$], precipitable water [$w(d)$], and albedo [$\alpha(d)$] inputs for two different broadband solar radiation routines. To avoid problems with unknown underlying distributions in the data and inherent heteroscedasticity, generalized least-squares regression (GLS a.k.a. 'weighted') analyses were used for the $\sigma_a(d)$ depth and $w(d)$. Heteroscedasticity is most commonly characterized by nonconstant standard error of the regression estimate, but there are many other important statistical issues involved with this property (e.g., see Carroll and Ruppert, 1988). Ordinary least squares regressions (OLS) were used with the $\alpha(d)$ data. In each regression analysis, several diagnostics, including residual analyses, were examined.

3.1. Broadband model selection

The first solar radiation model, hereafter called 'model 1', was based on the model of Bird and Hulstrom (1981). It includes some of the modifications by NRSDB (NREL, 1995) and some proposed by Iqbal in his broadband model 3 (Iqbal, 1983). Iqbal (1983) and Bird and Hulstrom (1981) argue that this model compares well with various spectral models. The basic equation for total clear sky global radiation [direct (R_b) + diffuse (R_d)] was

$$R_{s,c} = I_0 \cos(Z) T_o T_g T_w \left\{ T_R T_a + 0.79 T_{a,a} \left[0.5(1 - T_R) + F_c(1 - T_{a,s}) \right] (1 - m + m^{1.02})^{-1} \right\} (1 - r_s \alpha)^{-1}$$

where the transmission equations[3] and associated parameters are: $m = (\cos(Z) + 0.50572(96.07995 - Z)^{-1.6364})^{-1}$; $m_r = mP/P_0$; $T_R = \exp[-0.0903 m_r^{0.84}(1 + m_r - m_r^{1.01})]$; $U_o = l_o m_o$; $T_o = 1 - 0.1611 U_o(1 + 139.48 U_o)^{-0.3035} - 0.002715 U_o(1 + 0.044 U_o + 0.0003 U_o^2)^{-1}$; $U_w = w m_r$; $T_w = 1 - 2.4959 U_w[(1 + 79.034 U_w)^{0.6828} + 6.385 U_w]^{-1}$; $T_a = \exp(-\sigma_a m)$; $T_{a,a} = 1 - (1 - w_0)(1 - m + m^{1.06})(1 - T_a)$; $T_{a,s} = T_a / T_{a,a}$; $r_s = 0.0685 + (1 - F_c)(1 - T_{a,s})$.

The air mass equation was from Kasten and Young (1989). The optical path for ozone and the dimensionless water vapor absorption were from Iqbal (1983). While Iqbal (1983) had seasonally varying norms for total ozone thickness, U_o, a constant value of 0.3 cm was used because the variation was small compared to other factors. As in Bird and Hulstrom (1981) and Iqbal (1983), the single scattering albedo, w_0, was set to 0.91. The ratio of forward to total aerosol scattering, F_c, was set to 0.82 (rural setting). Therefore, model 1 has direct beam irradiance that includes the effects of Rayleigh scattering and absorption by ozone, water vapor, permanent gases, and aerosols. It also has diffuse irradiance due to single Rayleigh scattering, aerosol absorption and scattering, and a correction factor for multiple surface reflections of single scattered radiation. Model 1 was chosen because it contains physically-based terms comparable to a reasonably comprehensive spectral model.

The second solar radiation model, hereafter called 'model 2', was based on the modifications of Bird and

[3] In this paper, T represents transmittance functions instead of air temperature which it normally denotes in this journal. Similarly, when m appears in a function it is for optical air mass and not for meter.

Hulstrom (1981) to the model of Atwater and Brown (1974). It has been employed in several studies by Atwater and Ball (Atwater and Ball, 1976, 1978a,b, 1981) and reportedly is valid for very clear atmospheric conditions (Bird and Hulstrom, 1981). The basic equation for global radiation ($R_b + R_d$) was

$$R_{s,c} = I_0 \cos(Z)[T_M - a_w]T_a(1 - r_s \alpha)^{-1}$$

where the transmission equations and associated parameters are: $m = 35(1224\cos^2(Z) + 1)^{-0.5}$; $m_r = mP/P_0$; $T_M = 1.021 - 0.0824(m(949 \times 10^{-5}P + 0.051)^{0.5})$; $a_W = 0.077(U_w m_r)^{0.3}$; $T_a = \exp(-\sigma_a m)$.

Model 2 uses Rodgers' air mass model (Rodgers, 1967) but with absolute air mass instead of relative air mass in the aerosol transmission component, so it was consistent with the corresponding term in model 1. Hence model 2, as parameterized, includes direct and diffuse irradiance. It accounts for effects due to aerosols and due to molecular absorption effects except water vapor. Water vapor absorptance is included separately. Also it has a factor for multiple surface reflections of single scattered radiation. Model 2 was chosen because it has few specific parameterizations and provides a good contrast to model 1.

Solar constant, equations of time, and solar hour angle were developed according to Iqbal (1983) and were the same for both models. Hour angle was centered in the 1-h time intervals including sunrise and sunset hours. For the purpose of this paper, adjusting the photoperiod and centering the hour angle in the sunrise and sunset photoperiod would be of little gain because the resulting bias in both daily solar radiation model estimates were both median bias error < 0.01 MJ m^{-2} based on Ames normal conditions. The maximum bias was $< |0.25|$ MJ m^{-2}. Maximum bias values were associated with extremes in the yearly variation of the equation of time. Daily totals were the sum of hourly values throughout the period of sunshine. Aside from σ_a, w, and α, the remaining inputs depended on the geographic coordinates. Standard atmospheric pressure and absolute air mass were adjusted for elevation via the hypsometric equation.

3.2. Aerosol optical depth analyses

A comparison of monthly Linke turbidity factor (T_n) constructed from the σ_a and w values for the Tucson SAMSON site (WBAN 23160) with the long-term T_n observations (27 years) of Zymber and Sellers (1985) at the nearby University of Arizona revealed no significant systematic differences (unpublished research). Therefore, the daily σ_a and w data for the chosen sites in this paper were directly used without any adjustment. Median values of aerosol optical depth were determined over all years by each day within the year and then used to represent the normal value, $\sigma_{a,nrm}(d)$. Similarly, corresponding minimum values were used to represent the climatic lower boundary, $\sigma_{a,min}(d)$. Fourier series and other suitable nonlinear candidate models for GLS regressions were used to develop annual trends. For each radiometer site selected, regression models were used to estimate the normal and minimal predictions along with the 95% confidence limits.

3.3. Precipitable water analyses

Precipitable water data extraction for each site paralleled that for aerosol optical depth. Similarly, medians represent normal precipitable water, $w_{nrm}(d)$, and minima represent the climatic lower boundary, $w_{min}(d)$. Again, GLS regression methodology was employed. Candidate models included Gaussian forms (bell-shaped) as well as Fourier series.

3.4. Albedo analyses

Since only mean monthly values were available and statistical uncertainty was not reported, ordinary least squares (OLS) methodology was used for the albedo regression analyses. The middle day of the month was used for the time coordinate. To track the shape in the albedo scatter plots for each site (which have high values in the winter and low values in the summer), models considered included Fourier series and splined polynomials.

3.5. Broadband model analyses

To test the potential clear day model predictions of the climatic upper boundary at each site, maximum values determined for each day in the year over the entire period of record were used $[R_{s,max}(d)]$; hereafter, these data are called the 'selected observations'. A summary of what the selection procedure captured will precede an assessment of the modeling. For each site, the selected data were subtracted from the model 1 and 2 predictions with three variations on σ_a and w: (1) the 'normal' curves for each were used (i.e., $\sigma_{a,nrm}(d)$ and $w_{nrm}(d)$); (2) the climatic 'minimum' curves for each were used (i.e., $\sigma_{a,min}(d)$ and $w_{min}(d)$); and (3) the 95% lower confidence limit for each of the minimum curves were used (i.e., $\sigma_{a,l1}(d)$ and $w_{l1}(d)$). The latter case was designated 'LL1'. For each site, univariate statistics for each of the differences were calculated. In addition, a simple error analysis for each of the inputs, α included, was conducted to assess the systematic variation in broadband predictions due to systematic differences in each of the input component estimates. For the Ames normal case, errors for each were set $\Delta\sigma_a = 0.01$; $\Delta w = 1$ mm; and $\Delta\alpha = 0.1$. Again univariate statistics for each variable were calculated.

Finally, for each model with a reselection from the selected data for the clearest day data from all three rural primary SAMSON sites, a more robust assessment analysis was done. For a 'reselected' set and predictions for each model from the climatic 'minimum' parameterization, the plot of Berg (1992) along with time residual plots and analyses, the Pearson correlation coefficient, and a combination of other statistics suggested by Fox (1981) and Willmott (1982) were used to assess the bounding of the observations by each model. The other statistics were: both variable means, mean bias error (bias), mean absolute error (MAE), root mean square error (RMSE), variance of the bias (s_d^2), and OLS linear regression analysis. There was, however, a major difference for Willmott's statistics; observations were treated as the dependent variable. This choice was made because the observations contained random errors. In contrast, model predictions were independent of random errors because inputs were all based only on time trend regressions. Model predications only have systematic errors. These analyses are generally intended to confirm that models adequately interpolate observations with a one-to-one relationship. A constant negative bias from this relationship, however, serves as a measure of distance from the upper boundary.

4. Results and discussion

The $\sigma_a(d)$ and $w(d)$ models and results are presented in Sections 4.1 and 4.2 and in Table 2. The final weight models for $\sigma_a(d)$ and $w(d)$ generally corresponded to a log-normal residual distribution or one intermediate between the Poisson and log-normal (the GLS regressions required two to three iteration cycles on the weight model). The $\alpha(d)$ models are given in Table 3 and analysis in Section 4.3. Bounding statistics are listed in Tables 4 and 5 and analyses are reported in Section 4.4.

4.1. Aerosol optical depth (σ_a)

In all cases, the $\sigma_a(d)$ curves (Table 2, section a) were best modeled with a simple sinusoid and the normal curves were nearly identical to NREL's corresponding monthly mean based model with the average parameter agreement being within a few percent (Appendix B, Table B1 of NREL, 1995). The worst regression and overall disagreement was for the Dodge City site. The data scatter was comparatively larger than that for any other site, the constant was 6% smaller (the second largest difference for this parameter), the amplitude coefficient was 25% smaller, and the phase angle (which was fit not fixed) was 14% larger. The Ames normal model was compared to the one NREL listed for Des Moines [41.52°N, 93.65°W, and 294 m elevation (Appendix B, Table B1 of NREL, 1995)]. The distance between Ames and Des Moines is about 60 km ($\approx 0.54°$ latitude). The Ames amplitude parameter was 14% higher than the one for Des Moines, while the mean was

Table 2
Regression component models tested in the broadband clear day routine

Site	n^a	R^2	Model[b]	Weight model[c]
Aerosol optical depth models, σ_a				
Akron/Canton	365	0.80	median: $\sigma_{a,nrm}(d) = 0.123 + 0.042\cos((2\pi 365^{-1})(d-183))$	$s^2 = \hat{y}^2$
	365	0.93	minimum: $\sigma_{a,min}(d) = 0.060 + 0.021\cos((2\pi 365^{-1})(d-184))$	$s^2 = \hat{y}^2$
Ames	365	0.98	median: $\sigma_{a,nrm}(d) = 0.110 + 0.051\cos((2\pi 365^{-1})(d-189))$	$s^2 = \hat{y}^2$
	365	0.86	minimum: $\sigma_{a,min}(d) = 0.062 + 0.030\cos((2\pi 365^{-1})(d-191))$	$s^2 = \hat{y}$
Bismarck	365	0.96	median: $\sigma_{a,nrm}(d) = 0.071 + 0.030\cos((2\pi 365^{-1})(d-185))$	$s^2 = \hat{y}^4$
	365	0.83	minimum: $\sigma_{a,min}(d) = 0.029 + 0.012\cos((2\pi 365^{-1})(d-187))$	$s^2 = \hat{y}^{5/2}$
Columbia	360	0.97	median: $\sigma_{a,nrm}(d) = 0.100 + 0.042\cos((2\pi 365^{-1})(d-187))$	$s^2 = \hat{y}^{3/2}$
	352	0.88	minimum: $\sigma_{a,min}(d) = 0.043 + 0.020\cos((2\pi 365^{-1})(d-189))$	$s^2 = \hat{y}^4$
Dodge City	357	0.30	median: $\sigma_{a,nrm}(d) = 0.072 + 0.031\cos((2\pi 365^{-1})(d-208))$	$s^2 = \hat{y}^{3/2}$
	365	0.91	minimum: $\sigma_{a,min}(d) = 0.031 + 0.017\cos((2\pi 365^{-1})(d-191))$	$s^2 = \hat{y}^2$
Precipitable water models, w				
Akron/Canton	365	0.98	median: $w_{nrm}(d) = 0.67 + 2.20\exp(-0.000144(d-207)^2)$ cm	$s^2 = \hat{y}^{3/2}$
	365	0.96	minimum: $w_{min}(d) = 0.35 + 1.42\exp(-0.000138(d-208)^2)$ cm	$s^2 = \hat{y}^{3/2}$
Ames	365	0.98	median: $w_{nrm}(d) = 0.64 + 2.48\exp(-0.000145(d-204)^2)$ cm	$s^2 = \hat{y}$
	365	0.92	minimum: $w_{min}(d) = 0.27 + 1.53\exp(-0.000157(d-204)^2)$ cm	$s^2 = \hat{y}^2$
Bismarck	365	0.98	median: $w_{nrm}(d) = 0.47 + 1.88\exp(-0.000154(d-204)^2)$ cm	$s^2 = \hat{y}$
	365	0.94	minimum: $w_{min}(d) = 0.17 + 1.19\exp(-0.000198(d-205)^2)$ cm	$s^2 = \hat{y}$
Columbia	365	0.96	median: $w_{nrm}(d) = 0.72 + 2.73\exp(-0.000141(d-204)^2)$ cm	$s^2 = \hat{y}^{3/2}$
	362	0.87	minimum: $w_{min}(d) = 0.25 + 1.43\exp(-0.000155(d-203)^2)$ cm	$s^2 = \hat{y}^2$
Dodge City	365	0.98	median: $w_{nrm}(\mathrm{d}) = 0.61 + 2.30\exp(-0.000163(d-205)^2)$ cm	$s^2 = \hat{y}^{3/2}$
	365	0.91	minimum: $w_{min}(\mathrm{d}) = 0.27 + 1.41\exp(-0.000195(d-207)^2)$ cm	$s^2 = \hat{y}^{3/2}$

[a]Most data sets had at least one outlier. In the regressions, observations with weighted residuals that were outliers at the $P < 0.001$ level were removed when there were three or more, and then the regression was redone.
[b]All parameters have $P < 0.01$ or better based on their T value.
[c]The weight models are for inverse variance weighting, i.e., weight $= 1/s^2$. Here s^2 is the variance and $\hat{y}$ is the predicted value.

10% higher, and the phase angle date was 3% higher. Since parameter standard errors were not reported for any location, more formal statistical comparisons were not done. The agreement, however, seems reasonable considering that the normal model in this study was developed differently from those listed in Appendix B, Table B1 of NREL (1995). The daily median-based data selection procedure used in this study along with the weighted regressions should, in general, be a more robust methodology than NREL's. NREL used OLS on monthly means (Chapter 6 of NREL, 1995). The climatic minimum curves fit very well, and were developed similarly. Hence the GLS models developed in this work were utilized for $\sigma_{a,nrm}(d)$ curves rather than NREL's models. Typical results, as shown in Fig. 1, have the climatic normal distinct from the climatic minimum throughout the annual cycle ($P < 0.05$). The occasional overlapping of the 95% confidence limits for some periods occurred within the annual cycle for both the σ_a and w comparisons. In any of these cases, however, the curves can be made distinct throughout the annual cycle by relaxing the P level, generally to $P \approx 0.1$.

Error differences (sometime called 'sensitivity') were not constant throughout the year (they were largest at or near the summer solstice and smallest in the winter). Model 2 error differences were comparatively larger than those for the corresponding model 1 results. On the average, a decrease of 0.01 from the normal σ_a increased the average daily solar radiation estimate by 0.09 MJ m^{-2} in model 1 and 0.35 MJ m^{-2} in model 2; so model 2 is about 4 times as sensitive to changes in σ_a as model 1! This result is difficult to show analytically because $d(\text{model } 1)/d\sigma_a$ is a highly nonlinear expression but $(d(\text{model } 1)/d\sigma_a)/(d(\text{model } 2)/d\sigma_a)$ can be evaluated on any time scale and over any period numerically. An analytic expression for the absolute value of this ratio was developed for use with the Ames normal model. On any given day the value of the hourly ratio varied throughout the day generally reaching a maximum at noon with an average value of 0.285 but ranged

Table 3
Albedo models used in the broadband clear day routine

Site	n	R^2	Model[a]
Ames	12	0.997	$\alpha(d)=\begin{cases}0.612+2.45\cdot10^{-3}d-5.60\cdot10^{-5}d^2, & d\le116\\ 0.140, & 116<d\le284\\ 0.140+0.0112(d-284)-5.92\cdot10^{-5}(d-284)^2, & d>284\end{cases}$
Bismarck	12	0.995	$\alpha(d)=\begin{cases}0.660, & d\le74\\ 0.660-0.0608(d-74), & 74<d\le153\\ 0.180, & 153<d\le256\\ 0.180+0.0927(d-256)-4.30\cdot10^{-5}(d-256)^2, & d>256\end{cases}$
Columbia	12	0.999	$\alpha(d)=\begin{cases}0.596+1.19\cdot10^{-3}d-4.76\cdot10^{-}5d^2, & d\le111\\ 0.140, & 111<d\le287\\ 0.140+9.56\cdot10^{-3}(d-287)-4.68\cdot10^{-5}(d-287)^2, & d>287\end{cases}$
Dodge City	12	0.996	$\alpha(d)=\begin{cases}0.651-3.29\cdot10^{-5}d, & d\le120\\ 0.180, & 120<d\le285\\ 0.180+0.0103(d-285)-5.16\cdot10^{-5}(d-285)^2, & d>285\end{cases}$
Wooster	12	0.999	$\alpha(d)=\begin{cases}0.537+1.38\cdot10^{-3}d-3.73\cdot10^{-5}d^2, & d\le114\\ 0.213, & 114<d\le284\\ 0.213+3.47\cdot10^{-3}(d-284)-5.52\cdot10^{-6}(d-284)^2, & d>284\end{cases}$

[a]All parameters have $P<0.1$ or better based on their T value.

from 0.069 excluding sunrise and sunset hours. The daily value was not as varied throughout the year and had a median value of 0.259 which is about 0.09/0.35. More complicated sensitivity analyses for all inputs were conducted but revealed little additional insight. Errors in the component inputs were obviously additive.

4.2. Precipitable water (w)

Gaussian regression models for the normal and minimum w trends were selected because in each case they interpolated the data better than sine curves (Table 2, section b), as the Wooster curves and data show (Fig. 2). Again, generally the climatic normals were distinct from the climatic lows ($P<0.05$).

As with the σ_a errors, prediction differences were not constant throughout the year (they were largest during early spring and smallest during midsummer) and model 2 differences were somewhat larger than those for the corresponding model 1 results. The magnitude of these differences was smaller than any of those for $\sigma_a(d)$. A decrease of 1 mm from the normal $w(d)$ increased the average daily solar radiation estimate by 0.04 MJ m^{-2} in model 1 and 0.05 MJ m^{-2} in model 2.

4.3. Surface albedo (α)

Splined polynomial regression models were selected as the best means to interpolate the α data for all sites, although the fits in the early part of the year were not as good as those for the rest of the year. The Ames curve and data were typical (Fig. 3). Based on normal snowfall, air temperature, and cropping patterns for central Iowa, the Ames model and data seemed reasonable (Waite and Hillaker, 1982; ISU, 1986). Furthermore, as will be discussed in the next paragraph, the broadband models are not very sensitive to the α estimate. In some versions of both models the $(1-r_s\alpha)^{-1}$ is left out. Nonetheless, little variation is shown during the growing season in Fig. 3. In an unpublished examination of 1 km^5 surface albedo data derived from satellite remote sensing data composited every two weeks and covering the state of Iowa throughout the period from April

Table 4
Comparison of differences between selected observations and predictions from several clear day model parameterizations[a]

Comparison[b]	Site	Absolute		Relative			Predicted < Observed (%)
		MAE (MJ m^{-2})	MBE (MJ m^{-2})	MBE(%)	MAX(%)	MIN(%)	
Model 1							
Normals	Ames	1.12	−0.88±0.06	−5.71±0.40	0.75 (58)	−31.73 (347)	78.5
	Bismarck	0.56	0.51±0.02	2.76±0.13	11.19 (323)	−3.65 (5)	10.7
	Columbia	0.43	0.17±0.03	1.32±0.14	10.53 (362)	−5.41 (142)	33.4
	Dodge City	0.44	0.32±0.02	1.73±0.11	8.08 (338)	−3.44 (132)	21.4
	Wooster	1.10	0.00±0.07	−1.35±0.27	15.01 (357)	−40.45 (356)	47.5
Minima	Ames	0.99	−0.11±0.06	−1.96±0.39	10.84 (182)	−27.07 (347)	50.8
	Bismarck	1.39	1.39±0.04	6.95±0.13	15.33 (323)	0.90 (5)	0
	Columbia	1.34	1.34±0.03	6.31±0.13	14.83 (362)	0.11 (142)	0
	Dodge City	1.20	1.20±0.02	5.43±0.11	11.82 (338)	0.10 (84)	0
	Wooster	1.43	0.80+0.08	2.30±0.43	18.45 (357)	−34.76 (356)	27.6
LL1	Ames	1.08	0.25±0.07	−0.36±0.39	12.45 (182)	−25.24 (347)	40.1
	Bismarck	1.71	1.71±0.04	8.49±0.13	16.98 (323)	2.85 (130)	0
	Columbia	1.78	1.78+0.03	7.99±0.12	16.00 (362)	2.18 (142)	0
	Dodge City	1.54	1.54+0.03	6.79±0.11	13.13 (338)	1.52 (89)	0
	Wooster	1.56	1.00±0.08	3.21±0.42	19.31 (357)	−33.35 (356)	24.9
Model 2							
Normals	Ames	2.58	−2.57+0.06	−14.69±0.42	1.65 (58)	−42.39 (347)	99.7
	Bismarck	0.84	−0.81±0.04	−3.97±0.14	4.61 (323)	−10.32 (134)	92.3
	Columbia	1.86	−1.85±0.06	−8.54+0.21	3.09 (362)	−18.33 (174)	98.6
	Dodge City	0.99	−0.91±0.04	−3.81±0.17	3.34 (86)	−10.67 (237)	84.7
	Wooster	1.95	−1.90±0.07	−11.29±0.49	7.22 (64)	−54.35 (356)	93.9
Minima	Ames	1.08	−0.82±0.06	−5.17±0.38	9.09 (58)	−30.18 (347)	76.2
	Bismarck	1.34	1.34±0.03	7.08±0.14	16.00 (323)	1.03 (134)	0
	Columbia	0.96	0.94±0.02	4.96±0.16	15.05 (362)	−2.68 (174)	3.6
	Dodge City	1.11	1.11±0.02	5.39±0.14	13.02 (338)	−0.32 (132)	0.8
	Wooster	1.10	0.12±0.07	−0.69±0.43	16.43 (357)	−38.13 (356)	44.2
LL1	Ames	0.94	−0.08±0.06	−1.62±0.37	11.63 (58)	−25.74 (347)	50.8
	Bismarck	1.92	1.92±0.04	9.72±0.14	17.84 (323)	3.61 (134)	0
	Columbia	1.76	1.76±0.03	8.05±0.13	16.81 (362)	1.88 (142)	0
	Dodge City	1.69	1.69±0.02	7.66±0.14	15.06 (338)	2.10 (138)	0
	Wooster	1.25	−0.51±0.08	1.13±0.43	18.03 (357)	−35.49 (356)	32.9

[a]MAE: median bias error; MBE: mean bias error; MAX: maximum (value in parentheses is the day in the year the maximum was realized); MIN: minimum (value in parentheses is the day in the year the minimum was realized).
[b]Comparison parameterizations (for 365 observations at all but Wooster which had 362). Normals: $R_{s,max}(d) - R_{s,c}(\sigma_{a,nrm}(d), w_{nrm}(d), \alpha(d))$ in MJ m^{-2}; Minima: $R_{s,max}(d) - R_{s,c}(\sigma_{min}(d), w_{min}(d), \alpha(d))$ in MJ m^{-2}; LL1: $R_{s,max}(d) - R_{s,c}((\sigma_{a,l11}(d)\ w_{l11}(d), \alpha(d))$ in MJ m^{-2}.

through September in 1990 (there was no snow cover throughout the given period), mean albedo data ranged from approximately 0.14 to 0.20 and roughly increased with time. The crop growth patterns in 1990 were reasonably normal. Hence, if operational considerations of a chosen model allow for the input of albedo data, and if better or locally derived estimates are available, they could be used.

Error analysis results were similar to those for the σ_a input but smaller in magnitude, making α the least consequential component in the models. An increase of 0.1 from the normal $\alpha(d)$ increased the average daily solar radiation estimate by 0.20 MJ m^{-2} in model 1 and 0.13 MJ m^{-2} in model 2. In each model this comparative difference in the predicted daily values (due to the increase in α) usually meant less than a 1% change.

Table 5
Quantitative measures of clear day global solar radiation model performance[a]

Model[b]	N	$\overline{O}$	$\overline{P}$	Ratio	r	MAE	RMSE	Bias	s_d^2	b_0	b_1	SEE	PRESS
1	54	20.92	21.75	0.962 ($P < 0.0001$)	0.999	0.826	0.939	-0.826 ± 0061	0.202	-0.501 ± 0.174	0.984 ± 0.008	0.44	10.82
											0.965 ± 0.003	0.47	12.14
2	54	20.92	21.60	0.969 ($P < 0.0001$)	0.998	0.727	0.849	-0.681 ± 0.070	0.262	-1.021 ± 0.204	1.016 ± 0.009	0.50	14.23
											0.974 ± 0.004	0.61	20.35

[a]Observations are selected from all sites. Model inputs are for climatic minima in aerosol optical depth and precipitable water.
[b]N: number of observations; $\overline{O}$: mean observed value of maximum clear day measurements $[R_{s,max}(d)]$ in MJ m^{-2}; $\overline{P}$; Mean predicted value of maximum clear day measurements $[R_{s,c}(d)]$ in MJ m^{-2}; Ratio: (mean observed)/(mean predicted); r: Pearson product-moment correlation coefficient; MAE: mean absolute error (MJ m^{-2}); RMSE: root mean square error (MJ m^{-2}); Bias: mean bias error (MJ m^{-2}); S_d^2: bias variance; b_0: intercept estimate in the ordinary least squares regression model $R_{s,max}(d) = b_0 + b_1 R_{s,c}(d)$, with the standard error of the parameter estimate; b_1: line 1: slope estimate in the ordinary least squares regression model $R_{s,max}(d) = b_0 + b_1 R_{s,c}(d)$, with the standard error of the parameter estimate; line 2: slope only estimate in the ordinary least squares regression model $R_{s,max}(d) = b_1 R_{s,c}(d)$, with the standard error of the parameter estimate; SEE: standard error of the regression estimate (MJ m^{-2}); PRESS: prediction error sum of squares.

4.4. Clear day solar radiation ($R_{s,c}$)

For each site, the selection procedure of each maximum daily R_s datum $[R_{s,max}(d)]$ from the 30-year record does not necessarily yield an observation that lies on the climatic clear day boundary. While it is not known what the relevant ambient meteorological conditions were for a datum that the selection process chose for Ames and Wooster sites, R_s, w, and σ_a were known for the chosen SAMSON sites. The SAMSON site $R_{s,max}(d)$ data were generally, but not exclusively, from very low total sky cover (tsc) days. For the Bismarck, Columbia, and Dodge City SAMSON sites collectively, 51% of the selected data had a tsc < 0.05, 65% < 0.10, 82% < 0.20, and 90% < 0.30. The correlation between tsc and $R_{s,max}(d)$ was insignificant at any reasonable probability level.

A common date for the selection of maximum R_s, minimum w, and minimum σ_a was rare. Bismarck had 10 such observations, the other two had 22 each. Collectively, these amounted to 4.9% of the selected data. This

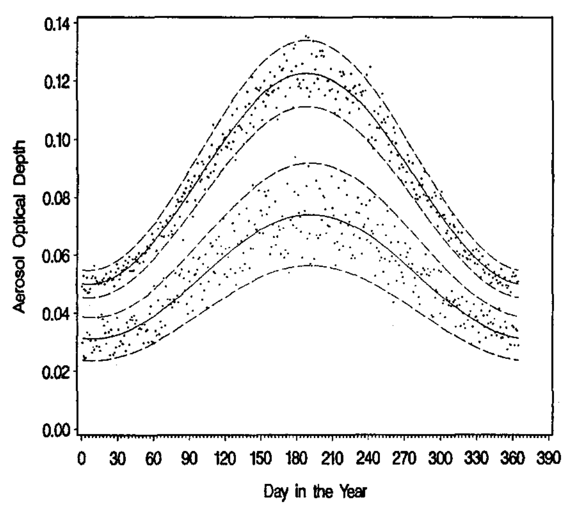

Fig. 1. Normal (upper set, solid square) and minimum (lower set, solid circle) aerosol depth data and annual trend models with 95% confidence limits for Ames, IA. Data were for the period 1961–1990. Regression results are listed in Table 2.

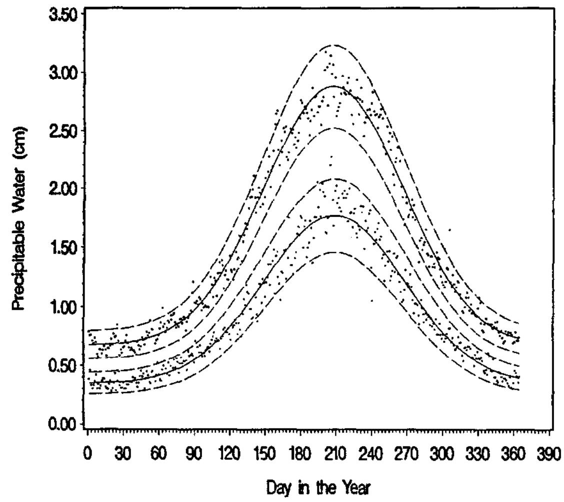

Fig. 2. Normal (upper set, solid square) and minimum (lower set, solid circle) precipitable water data and annual trend curves with 95% confidence limits for Akron/Canton, OH. Data were for the period 1961–1990. Regression results are listed in Table 2.

subset is designated the 'reselected' data. It is admittedly not an independent confirmation set and has the same kinds of problems but to a lesser extent.

In all of the sites the selected $R_{s,max}(d)$ data were skewed in time toward the first two decades of the period of record. Ames and Wooster, however, were comparatively much more so. For the Bismarck, Columbia, and Dodge City SAMSON sites collectively, 63% of the data were drawn from the first half of the period of record and 79% from the first two decades. The corresponding values for Ames were 89% and 97%; those for Wooster were 75% and 87%. In the Ames selected data, over a week of sequential observations from the mid-1960s well exceeded extraterrestrial values and so were replaced with the next highest observation. Wooster only had three such points, therefore they were just deleted.

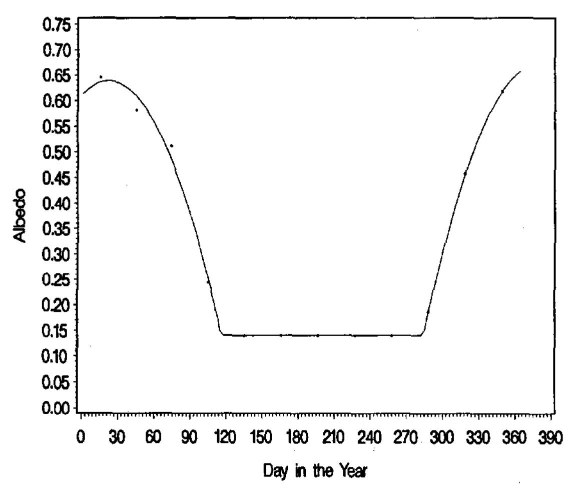

Fig. 3. Monthly mean albedo data and annual trend curve for Ames, IA. Data were for an unspecified period. Regression results are listed in Table 3.

The $R_{s,max}(d)$ data selection was repeated for the Akron/Canton secondary SAMSON site and compared to the set for Wooster. The Wooster data were on the average 1.25 MJ m^{-2} higher. Comparing the scatter plots for the chosen SAMSON sites to those from Ames and Wooster reveals that the latter are much more scattered and probably not of the same quality. Data outside of the SAMSON database are likely not to be of the same quality.

Both broadband models using the climatic normal inputs underestimated the boundary for the selected observations. Model 1 estimates generally interpolated the data, while the model 2 estimates greatly underestimated the data (Table 4). The error analysis results suggest that model 2 is considerably more sensitive to σ_a. Therefore, the use of either model, especially model 2, with climatic normals is unsatisfactory. Perhaps data that fall below the model 1 curve should be excluded, since the selection procedure does not guarantee that a datum is truly in the clear day upper boundary population. For the Bismarck, Columbia, and Dodge City SAMSON sites collectively, the selected observations were bound by both the climatic minimum and LL1 inputs, although a few of the selected data were above the model 2 estimates from minimums for Columbia and Dodge City (Table 4). Results for Columbia were typical (Fig. 4). For Ames and Wooster, the assessment was more difficult because of greater data scatter and probable lower data quality; however, the prevailing trends were the same (Table 4). The data show that all of the observations that lie above the model 1 boundary for both the Ames and Wooster sites were highly skewed to the earlier part of the observation period. For Ames, 99.5% of the outliers were in the first two decades and 97.3% in the first 15 years; the comparative values for Wooster were 98.0% and 95.0%. Perhaps before the automation of the data acquisition and processing process, the methodology favored overestimation, particularly on clearer days. If so, the Ames and Wooster data could be adjusted to become more consistent with the rest. For all sites, the magnitude of the model/data difference was positively correlated with $R_{s,max}(d)$ (not constant throughout the annual period). The relative value of the differences behaved in the opposite way, but comparatively, the effect was greatly reduced. Based on climatic minimum in w and σ_a model 1 relative differences, the data for the SAMSON primary sites were bound on the average by 6.2% (1.3 MJ m^{-2}) and for model 2 by 5.8% (1.1 MJ m^{-2}); the corresponding values for the LL1 conditions were 7.8% (1.7 MJ m^{-2}) for model 1 and 8.5% (1.8 MJ m^{-2}) for model 2.

There is no general agreement or precedent on selecting the best model for bounding $R_{s,max}(d)$ data. Furthermore, although the long-term data come from high-precision radiometers, there are many possible problems with using such data for modeling and model confirmation (e.g., see Atwater and Ball's discussion (Atwater and Ball, 1978a) that includes radiometer calibration and drift problems). Both models and data are always questionable. Over the long run the very best data, such as my 'reselected data', are probably not better ± 1 MJ m^{-2} or 5%. So $+1$ MJ m^{-2} is proposed as a minimum condition for bounding the selected data, provided the boundary curve is otherwise satisfactory.

A choice between models 1 and 2 is not clear-cut and cannot be based on only one or two performance measures. Instead, a collective assessment should be made based on scatter plots, residual plots, and several different types of performance measures using both the selected data, but particularly the reselected data, because many of the selected data were probably not as good candidates for this task. For this analysis both models employed the climatic low inputs. Based on bias alone for the selected data, model 1 always exceeded the proposed value of 1 MJ m^{-2} but model 2 did not, for one case, Columbia. Based on bias alone for the reselected data, both models failed and each bias value was statistically different from 1 MJ m^{-2} ($P < 0.05$). Using all error measures, however, model 1 was reasonably close to $+1$ MJ m^{-2} while model 2 was not (Table 5 and Fig. 5). Other means of assessment considered were similar and comparatively very close (Table 5); in general favoring model 1 but not to the total exclusion of model 2 which, given its greater simplicity, can be a sound practical choice. If one desires to be more conservative, however, model 2 should be used with the LL1 inputs. Thus, with the availability of the SAMSON database, a reasonable and unambiguous definition (and model) for $R_{s,c}(d)$ is manifest. With model 1, it is the radiative transfer estimate, $R_{s,c}(d)$, using the climatic low trends in the turbidity parameters, $\sigma_{a,min}(d)$ and $w_{min}(d)$. For model 2, it is the $R_{s,c}(d)$ estimate using $\sigma_{a,LL1}(d)$ and $w_{LL1}(d)$.

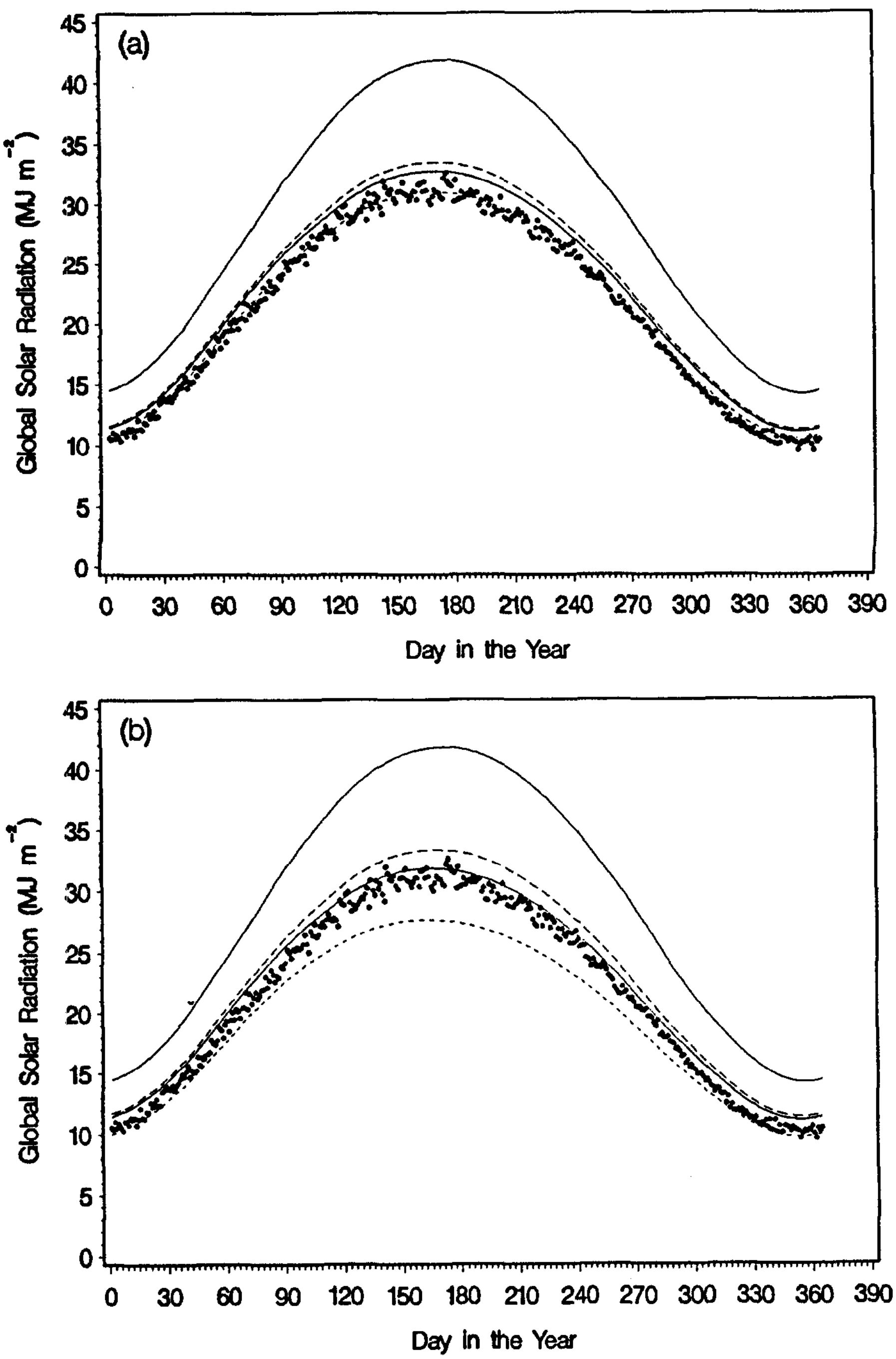

Fig. 4. Clear-day global solar radiation model results for Columbia, MO, model 1 in (a) and model 2 in (b). In each figure, the top solid line is for the extraterrestrial model, the upper broken line is for the LL1 inputs, the lower solid line is for the climatic low inputs, and the bottom broken line is for the climatic normal inputs. The solid circles are the selected clear-day data.

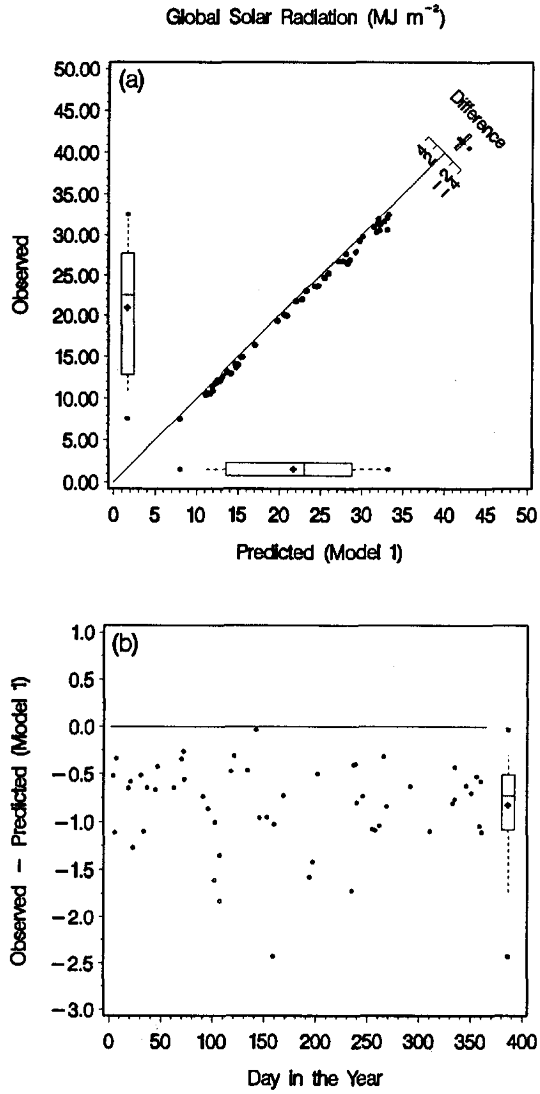

Fig. 5. (a) Berg (1992) plot for the reselected observations and the model 1 predictions for the climatic low input components. Summary statistics are listed in Table 5. (b) Differences of the observed and predicted values shown in (a) but plotted against day in the year.

Recall from the introduction that the SAMSON database was developed on an hourly time interval. The time base for the daily broadband models was also on an hourly interval. Most of the existing and developing micrometeorological station networks and hydrological studies store automated data on an hourly or subhourly basis. Therefore, future work developing and confirming an hourly-based $R_{s,c}$ is possible and could be useful for screening hourly R_s and directly estimating attenuation in an hourly net radiation model like that of Dong et al. (1992). A framework for this task needs to be planned first.

Finally, in practice, a metamodel for the $R_{s,c}(d)$ estimates for a given site could be developed and used in place of the $R_{s,c}(d)$ model. In this case a 'metamodel' is a regression of the broadband estimates on day in the year. Metamodels could then be used when computational simplicity, time, or costs are important.

5. Conclusion

When normal trend estimates of σ_a and w for each of two long-term radiometer stations were used to predict $R_{s,c}(d)$ with either one of two broadband solar radiation models, a systematic underestimation of the upper boundary resulted in each case with model 1 generally interpolating the selected data and model 2 generally completely underestimating them. Employing input component models developed from the climatic minima data for each site completely bounded all the selected data with model 1 and almost did so with model 2 but only for the chosen SAMSON sites. The Ames and Wooster data, which are probably systematically high and of lower quality, had similar patterns but had about half their observations above the boundary. Employing the lower confidence limits from the latter climatic input models (LL1 inputs) gave a more conservative boundary for both models at all sites.

The most influential component in both models was σ_a, while α was the least. For practical purposes, model 2, which is simpler, worked as well as model 1 for bounding the data. The methodology set a reasonable, reproducible, and unambiguous definition for $R_{s,c}(d)$ and can be used for better estimation of $R_{s,c}(d)$, particularly at locations throughout the United States that lack long-term radiometer data (e.g., many of the locations in the Cooperative Station Network, hydrological studies, etc.).

Acknowledgements

This work was supported by the USDA-ARS-MWA National Soil Tilth Laboratory (NSTL), Dr. J.L. Hatfield, Director. Prof. R.E. Carlson, ISU, Ames, IA, provided the Ames solar radiation data. Profs. J. Holeman and D. Elwell, OSU, Columbus, OH provided the Wooster solar radiation data and meteorological information. Prof. D.N. Yarger, ISU, Ames, IA, provided advice, encouragement, and comments on the manuscript. Prof. W.D. Sellers, UA, Tucson, AZ, provided comments on the manuscript. Dr. E.L. Maxwell, USDE-NREL, Golden, CO, provided comments on the manuscript and information on SAMSON. Dr. J. Prueger, USDA-ARS-MWA NSTL and anonymous reviewers also provided comments and advice. Mrs. J. Meek graciously edited the manuscript.

Appendix A. Definition of symbols

α	surface albedo (dimensionless fraction)
a_w	water vapor absorptance for model 2 (dimensionless fraction)
d	day in the year (integer day number, 1 to 365)
F_c	fraction of forward to total scattering (dimensionless)
I_0	solar constant in an hourly model (4.921 MJ m^{-2} [from 1367 W m^{-2}])
l_0	ozone layer thickness (cm)
m	relative optical air mass (dimensionless)
m_r	absolute (pressure corrected) optical air mass
m_o	ozone relative optical air mass
n	number of observations in a data set
P	atmospheric pressure (kPa)
P_0	standard atmospheric pressure (101.325 kPa)
R_b	direct solar radiation (MJ m^{-2})
R_d	diffuse solar radiation (MJ m^{-2})

r_s	sky albedo (dimensionless fraction)
R_s	global solar radiation (MJ m^{-2})
$R_{s,c}$	clear day global solar radiation (MJ m^{-2})
$R_{s,max}$	maximum R_s datum in the historical record for each d (MJ m^{-2})
σ_a	broadband aerosol optical depth (dimensionless or m^{-1})
$\sigma_{a,nrm}$	normal trend estimate of σ_a
$\sigma_{a,min}$	minimum trend estimate of σ_a
$\sigma_{a,lll}$	95% lower confidence limit for $\sigma_{a,min}$
T_a	transmittance of aerosols (dimensionless fraction)
T_{aa}	transmittance of aerosol absorptance (dimensionless fraction)
T_{as}	transmittance of aerosol scattering (dimensionless fraction)
T_g	transmittance of uniformly mixed gases (dimensionless fraction)
T_M	transmittance (global) of all molecular effects except water vapor for model 2 (dimensionless fraction)
T_n	Linke turbidity factor (Rayleigh atmospheres)
T_R	transmittance of Rayleigh scattering (dimensionless fraction)
T_o	transmittance of ozone absorptance (dimensionless fraction)
T_w	transmittance of water vapor absorptance (dimensionless fraction)
U_o	total optical path length for ozone (cm)
U_w	total optical path length for water vapor (cm)
w	precipitable water thickness (cm)
w_{nrm}	normal trend estimate of w
w_{min}	minimum trend estimate of w
w_{lll}	95% lower confidence limit for w_{min}
w_0	single-scattering albedo (dimensionless fraction)
Z	solar zenith angle (degrees or radians depending on the equation)

References

Ångström, A., 1924. Solar and terrestrial radiation. Quart. J. Roy. Meteorol. Soc. 50, 121–126.

Atwater, M.A., Ball, J.T., 1976. Comparisons of radiation computations using observed and estimated precipitable water. J. Appl. Meteorol. 15, 319–320.

Atwater, M.A., Ball, J.T., 1978a. Intraregional variations of solar radiation in the Eastern United States. J. Appl. Meteorol. 17, 1116–1125.

Atwater, M.A., Ball, J.T., 1978b. A numerical solar radiation model based on standard meteorological observations. Solar Energy 21, 163–170.

Atwater, M.A., Ball, J.T., 1981. A surface solar radiation model for cloudy atmospheres. Mon. Wea. Rev. 109, 878–888.

Atwater, M.A., Brown, P.S., 1974. Numerical computation of the latitudinal variations of solar radiation for an atmosphere of varying opacity. J. Appl. Meteorol. 13, 289–297.

Baker, D.G., Klink, J.C., 1975. Solar radiation reception, probabilities, and areal distribution in the North-Central Region. NCR Pub. 225 - Univ. MN Agric. Exp. Stn. Tech. Bull., 300, St. Paul, MN, 54 pp.

Berg, R.L., 1992. First place. Best presentation of data-Monochrome. Proc. 17th Annual SAS Users Group Int. Conf. Honolulu, HI. SAS Inst., Cary, NC, pp. 1521–1527.

Bird, R., Hulstrom, R., 1981. A simplified clear sky model for direct and diffuse insolation on horizontal surfaces. SERI/TR-642-761. US Department of Energy - NREL, Golden, CO, 38 pp.

Bland, W.L., Clayton, M.K., 1994. Spatial structure of solar radiation in Wisconsin. Agric. For. Meteorol. 69, 65–84.

Brutsaert, W.H., 1982. Evaporation into the atmosphere: Theory, history, and applications. D. Rediel, Boston, 299 pp.

Carroll, R.J., Ruppert, D.R., 1988. Transformation and weighting in regression. Chapman & Hall, New York, 249 pp.

Davies, J.A., Idso, S.B., 1979. Estimating surface radiation balance and its components. In: Barfield, B.J., Gerbes, J.F. (Eds.), Modification of the aerial environment of plants. American Society of Agricultural Engineering, St. Joseph, MI, pp. 183–210.

Dong, A., Grattan, S.R., Carroll, J.J., Prashar, C.R.K., 1992. Estimation of daytime net radiation over well-watered grass. Am. Soc. Civ. Eng. J. Irrig. Drain. Engr. 118, 466–479.

Fox, D.G., 1981. Judging air quality model performance: A summary of the AMS workshop on dispersion model performance. Bull. Am. Meteorol. Soc. 62, 599–609.

Flowers, E.C., McCormick, R.A., Kurfis, K.R., 1969. Atmospheric turbidity over the United States. J. Appl. Meteorol. 8, 955–962.

Hatfield, J.L., Fuchs, M., 1990. Evapotranspiration models. In: Hoffman, G.J., Howell, T.A., Solomonn, K.H. (Eds.), Management of farm irrigation systems. American Society of Agricultural Engineering, St. Joseph, MI, pp. 33–59.

Heermann, D.F., Harrington, G.J., Stahl, K.M., 1985. Empirical estimation of daily clear sky solar radiation. J. Clim. Appl. Meteorol. 24, 206–214.

Howell, T.A., Meek, D.W., Hatfield, J.L., 1983. Relationship of photosynthetically active radiation to shortwave radiation in the San Joaquin Valley. Agric. Meteorol. 28, 157–175.

Howell, T.A., Meek, D.W., Phene, C.J., Davis, K.R., McCormick, R.L., 1984. Automated weather data collection for research on irrigation scheduling. Trans. Am. Soc. Agric. Eng. 27, 386–391, 396.

Hummel, J.R., Reck, R.A., 1979. A global surface albedo model. J. Appl. Meteorol. 18, 239–253.

Iqbal, M., 1983. An Introduction to solar radiation. Academic Press, New York, 390 pp.

Iowa State University (ISU), 1986. Crop calendars and agroclimatic data for the Central Crop Reporting District of Iowa, AG-118. IA State Univ. Coop. Ext. Ser., Ames, IA, 20 pp.

Jensen, M.E., Burman, R.D., Allen, R.G. (Eds.), 1990. Evapotranspiration and irrigation water requirements. Am. Soc. Civ. Eng. manuals and reports on engineering practice, 70. American Society of Civil Engineers, New York, NY, 332 pp.

Kasten, F., Young, A.T., 1989. Revised optical air mass tables and approximation formula. Appl. Opt. 28 (22), 4735–4738.

Kustas, W.P., Goodrich, D.C., 1994. Preface, the MONSOON'90 multidisciplinary experiment. Water Resour. Res. 30 (5), 1211–1225.

Kung, E.C., Bryson, R.A., Lenschow, D.H., 1964. Study of continental surface albedo on the basis of flight measurements and structure of the earth's surface cover over North America. Mon. Wea. Rev. 92, 543–564.

Meek, D.W., Hatfield, J.L., 1994. Data quality checking for single station meteorological databases. Agric. For. Meteorol. 69, 85–109.

Meyer, S.J., Hubbard, K.G., 1992. Nonfederal automated weather stations and networks in the United States and Canada; a preliminary review. Bull. Am. Meteorol. Soc. 73 (4), 449–457.

Meyers, T.P., Dale, R.F., 1983. Predicting daily insolation with hourly cloud height and coverage. J. Clim. Appl. Meteorol. 22, 537–545.

National Renewable Energy Laboratory (NREL), 1992. NRSDB Vol. 1. User's Manual — National solar radiation data base (1961–1990). US Department of Energy-NREL, Golden, CO, 93 pp.

National Renewable Energy Laboratory (NREL), 1993. Users manual for the SERI QC Software: Assessing the quality of solar radiation data. US Department Of Energy - NREL, Golden, CO, 192 pp.

National Renewable Energy Laboratory (NREL), 1995. NRSDB Vol. 2. Final technical report — National solar radiation data base (1961–1990). US Department of Energy-NREL, Golden, CO, 260 pp.

Reber, E.E., Swope, J.R., 1972. On the correlation of total precipitable water in a vertical column to absolute humidity at the surface. Report TR-0172 (2230 20)-13. The Aerospace Corporation, POB 92957, Los Angeles, CA, 17 pp.

Rodgers, C.D., 1967. The radiative heat budget of the troposphere and lower stratosphere. Report No. A2. Dept. Meteorol. Planetary Circulations Project. MIT, Cambridge, MA, 99 pp.

Shuttleworth, W.J., 1993. Evaporation. Chapter 4. In: Maidment, D.R. (Ed.), Handbook of hydrology. McGraw-Hill, New York, pp. 4.1–4.53.

Snyder, R.L., Pruitt, W.O., 1992. Evaporation data management in California. Irrigation and drainage, saving a threatened resource — in search of solutions. Proc. Irrigation and Drainage Session at Water Forum 1992, Baltimore, MD. American Society of Civil Engineers, New York, NY, pp. 125–132.

Suckling, P.W., Hay, J.E., 1976. Modeling direct, diffuse, and total solar radiation. Atmos. 14, 299–308.

Tracy, C.R., Hammond, K.A., Lechleitner, R.A., Smith II, W.J., Thompson, D.B., Whicker, A.D., Williamson, S.C., 1983. Estimating clear-day solar radiation: An evaluation of three models. J. Therm. Biol. 8 (3), 247–251.

United States Department of Agriculture, 1994. Water quality research plan for management systems evaluation areas (MSEAs): An ecosystem management program. ARS-123. USDA-ARS and CSRS, Washington, DC, 45 pp.

United States Department of Energy (USDOE), 1978. On the nature and distribution of solar radiation. HCP/T2552-01 UC-59, 62, 63A. USDOE, Washington, DC, 256 pp.

Waite, P., Hillaker, H.J., 1982. Iowa snow climatology. Climatology of Iowa series No. 5. IA Dept. Agric.-State Clim. Ofc., Des Moines, IA, 39 pp.

Willmott, C.J., 1982. Some comments on the model performance. Bull. Am. Meteorol. Soc. 63, 1309–1313.

World Meteorological Organization (WMO), 1967. A note on climatological normals. Technical Note, 84. WMO, Geneva, 19 pp.

Zymber, R.J., Sellers, W.D., 1985. Atmospheric turbidity at Tucson, Arizona: Variations and their causes. J. Clim. Appl. Meteorol. 24, 725–734.